www.czasopisma.pan.pl PAN POLSKA AKADEMIA NAUK www.journals.pan.pl

Arch. Metall. Mater. **63** (2018), 3, 1547-1553

DOI: 10.24425/123846

Z. GLAVAS*#, A. STRKALJ*, K. MALDINI**, F. KOZINA*

EFFECT OF BISMUTH AND RARE EARTH ELEMENTS ON GRAPHITE STRUCTURE IN DIFFERENT SECTION THICKNESSES OF SPHEROIDAL GRAPHITE CAST IRON CASTINGS

Effects of additions of 0.00064, 0.001 and 0.0042 wt.% Bi on the graphite structure in the section thicknesses of 3, 12, 25, 38, 50, 75 and 100 mm of spheroidal graphite cast iron castings containing 2.11 wt.% Si and rare earth (RE) elements (Ce + La + Nd + Pr + Sm + Gd) in the range from 0.00297 to 0.00337 wt.% were analyzed in this paper. Addition of Bi was not necessary for obtaining high nodule count and nodularity higher than 80% in section thicknesses of 3, 12 and 25 mm. RE elements showed a beneficial effect on the nodule count and nodularity in these sections. Nodularity was below 80% in section thicknesses of 38, 50, 75 and 100 mm when Bi was not added. Detrimental effect of RE elements on graphite morphology in these sections was neutralized by adequate addition of Bi. Addition of 0.001 wt.% Bi (ratio of RE/Bi = 3.27) was enough to achieve nodularity above 80% in the section thickness of 38 mm. Nodularity was increased above 80% in section thicknesses of 50, 75 and 100 mm by addition of 0.0042 wt.% Bi (ratio of RE/Bi = 0.78). At the same time, Bi significantly increased the nodule count. Nodularity above 80% and the high nodule count in the section thicknesses of 75 and 100 mm were also achieved by using an external metallic chill in the mold. In this case, addition of Bi was not required.

Keywords: spheroidal graphite cast iron casting, graphite structure, bismuth, rare earth elements, microstructure

1. Introduction

Spheroidal graphite cast iron (SGCI), like gray and compacted graphite iron contains graphite particles in microstructure. But these particles in SGCI are not interconnected and have a nodular (spheroidal) shape. This shape of graphite particles is much more favorable for obtaining high mechanical properties than flake or compacted (vermicular) form. When graphite particles are present in spheroidal shape, the metal matrix has a higher continuity [1]. Moreover, crack propagation through graphitic cast iron is much more difficult if the graphite particles have a spheroidal shape.

In order to obtain high mechanical properties of SGCI, the proportion of non-nodular graphite forms in the microstructure must be as low as possible [2-4]. Graphite particles with sharp edges have a particularly adverse effect.

Chemical composition and cooling rate during solidification of the casting have a crucial influence on graphite structure. Mg is an effective spheroidizing element. Added in the proper amount it promotes the formation of spheroidal graphite during solidification of the casting. Excessive Mg contents may result in the formation of carbides during solidification of the casting, particularly in thin sections. On the other hand, subversive antinodularizing elements, such as Ti, As, Sn, Sb, Pb, Bi and Al prevent the formation of spheroidal graphite. The severity of the negative impact of each antinodularizing element on the form of graphite in SGCI can be seen from the antinodularizing (Thielman's) factor K_1 [3,5-7]:

$$K_1 = 4.4\ (\text{wt\% Ti}) + 2\ (\text{wt\% As}) + 2.4\ (\text{wt\% Sn}) + 5\ (\text{wt\% Sb}) + 290\ (\text{wt\% Pb}) + 370\ (\text{wt\% Bi}) + 1.6\ (\text{wt\% Al}) \quad (1)$$

Generally, the value of K_1 factor should be as low as possible (<1). Small addition of RE elements (primarily Ce and La) in combination with Mg results in increasing the nodule count and nodularity [6,8,9]. Detrimental effects of As, Sn, Sb, Pb, Bi and Al can be neutralized by proper addition of RE elements [6,7]. However, excessive amount of RE elements may cause carbides in thin sections and the formation of undesirable chunky and exploded graphite in thick sections [6,8,10,11-15].

Eq. (1) shows that the Bi has a very detrimental effect on graphite structure in SGCI. One study reported that the presence of only 0.003 wt.% Bi may cause the formation of very harmful intercellular flake or mesh graphite in 25 mm thick sample and the formation of spheroidal graphite is completely prevented when the Bi content exceeds 0.006 wt.% [16,17]. Other studies showed that only 0.001 wt.% Bi can prevent graphite spheroidization if Ti is present in the melt [18,19]. It is evident that the critical Bi content depends on the presence of other elements, which provides an opportunity for further research in this field.

* UNIVERSITY OF ZAGREB, FACULTY OF METALLURGY, ALEJA NARODNIH HEROJA 3, 44103 SISAK, CROATIA
** CROATIAN WATERS, ULICA GRADA VUKOVARA 220, 10000 ZAGREB, CROATIA
# Corresponding author: glavaszo@simet.hr

Detailed studies have shown that Bi can have a beneficial effect on graphite structure in SGCI if added in the proper amount in combination with other elements [3,6,7,11,20-25]. Different Bi compounds (such as Bi oxide, Bi sulfide) were found in inclusions detected in the center of the graphite nodules, which acted as nucleation sites for graphite [20]. This indicates that Bi strongly promotes nucleation of graphite. One study showed that the addition of 0.01 wt.% Bi resulted in increasing the nodule count in section thicknesses of 2, 3, 5 and 10 mm [20]. The high nodule count hinders the formation of carbides, which is very important for the production of carbide free thin wall SGCI castings.

Detrimental effects of RE elements on the graphite structure in thick SGCI castings can be neutralized by Bi [3,6,7,11,24,25]. Addition of Bi must be strictly adjusted to the content of RE elements and the section thickness of the casting, which is a demanding task. Different RE/Bi ratios were obtained in the literature. This indicates that there are many variables that affect the obtained results and provides an opportunity for further research in this field. Various intermetallic compounds, such as Ce_4Bi_3, $CeBi_3$, CeBi, Ce_3Bi, LaBi, La_4Bi_3 and La_5Bi_3 may form by reaction of Bi with RE elements and these compounds act as nucleation sites for graphite [11,24-28]. Accordingly, Bi at the same time neutralizes the harmful effects of RE elements and improves the nucleation potential of the melt. These conditions allow the formation of a larger number of smaller nodules. However, various undesirable graphite forms may occur if the Bi content is greater than required for the neutralization of RE elements.

The formation of austenite shell around the graphite nodules significantly affects their final shape in SGCI [10,11,29-32]. Decrease in cooling rate during solidification decelerates enveloping of graphite nodule by austenite shell. Long contact time of graphite nodule with the remaining melt during slow cooling results in an uneven growth and degeneration of nodule. As the contact time increases, degeneration of graphite increases, resulting in lower nodule count and nodularity. Moreover, slow cooling also promotes segregation of elements, such as Mn, Cr, Mo, Bi, Sb, Sn, Al, Pb, etc., in remaining melt [10,33]. In this case, the melting temperature of the liquid iron is reduced and the solidification time is extended, which additionally delays the envelopment of graphite nodule by austenite shell. Fast cooling during solidification results in fast enveloping of graphite nodule by austenite shell and reduces segregation [10,33]. In such conditions, graphite nodule is not in contact with the melt for a long time and retains a spheroidal shape.

In many cases, SGCI castings do not have a uniform thickness. They may consist of a thin, medium-thick and thick sections. It means that there are differences in cooling (solidification) rate between certain segments of the casting. It would be useful to investigate whether the addition of Bi and RE elements has a beneficial or harmful effect in such castings. This article deals with the influence of Bi and RE elements on the graphite structure, nodularity and nodule count in the SGCI casting containing thin, medium-thick and thick sections.

2. Experimental

The base iron was produced in a medium-frequency coreless induction furnace from the following raw materials: special low-manganese pig iron (the proportion was 50.0%), steel scrap containing a very low amount of carbide-forming and antinodularizing elements (the proportion was 20.0%) and ductile iron returns (the proportion was 30.0%). Commercial preconditioner (3.0 to 5.0 wt.% Al, 0.6 to 1.9 wt.% Ca, 3.0 to 5.0 wt.% Zr, and 62.0 to 69.0 wt.% Si) was added to the base iron in order to improve the nucleation potential and effect of inoculation.

Cored wire treatment was used for nodularization (graphite spheroidizing). The chemical composition of FeSiMg treatment alloy contained in the core of the wire was as follows: 29.0 wt.% Mg, 0.5 wt.% Ce, 0.2 wt.% La, 42.0 wt.% Si, 1.4 wt.% Ca, and 0.9 wt.% Al. Commercial inoculant (1.9 wt.% Al, 1.5 wt.% Ca, 2.2 wt.% Ba, and 67.0 to 72.0 wt.% Si) was added simultaneously in the amount of 0.6 wt.%. Targeted Si content in SGCI melt was between 2.0 and 2.2 wt.%.

SGCI melt was poured into five green sand molds to obtain stepped test castings with seven different section thicknesses: 3, 12, 25, 38, 50, 75, and 100 mm (Fig. 1). In order to produce a greater effect of inoculation, commercial inoculant (0.75 to 1.25 wt.% Al, 0.75 to 1.25 wt.% Ca,1.5 to 2.0 wt.% Ce, and 70.0 to 76.0 wt.% Si) in the amount of 0.2 wt.% was added to the melt stream during the pouring into the molds. Bi was not added to the first and second stepped test castings (STC 1 and STC 2). However, external metallic chill was used in the mold for STC 2 in order to increase the cooling rate of the section thicknesses of 75 and 100 mm. The third, fourth and fifth stepped test casting (STC 3, STC 4 and STC 5) were casted with the addition of various amounts of pure Bi (99.99 wt.%) in order to obtain different RE/Bi ratios. Targeted Bi contents are shown in Table 1. Bi was added to the melt stream simultaneously with inoculant.

TABLE 1

Targeted Bi contents

Stepped test casting (STC)	Targeted Bi contents, wt.%
STC 1	—
STC 2	(chill for the section thicknesses of 75 and 100 mm)
STC 3	0.0005
STC 4	0.001
STC 5	0.005

Optical emission spectrometry (OES) was used for determining the contents of C, Si, S, P, Mg, Mn, Cr, Mo, Ni, Cu, W and V) on samples taken just before pouring the melt into molds. Determination of the contents of Bi, Ce, La, Nd, Pr, Gd, Sm, Sb, Sn, Zr, Nb, Co, As, Pb, Ca, Y, Ti, Cd and Al was performed using inductively coupled plasma mass spectroscopy (ICP-MS). Samples for this analysis were taken from the stepped test castings.

The microstructure of the central part of each section (Fig. 1) was analyzed using a light metallographic microscope with a digital camera and an image analysis system. Determina-

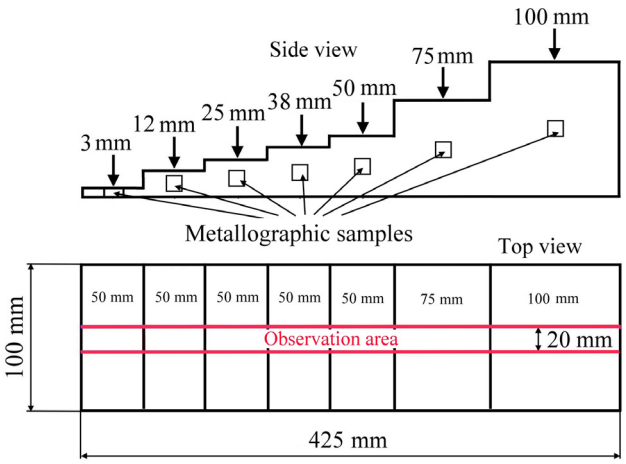

Fig. 1. Schematic show of the stepped test castings and places of taking samples for metallographic examinations

tion of nodularity and the nodule count was done in accordance with ASTM E2567-14 standard [34]. The classification of each graphite particle was carried out on the basis of its roundness-shape factor (SF = Area of graphite particle/Area of reference circle, where Area of reference circle = $\pi \cdot (\text{max. Feret})^2/4$). If the graphite particle had SF > 0.625, it was classified as a nodule. Carbides that were present in the thinnest section were analyzed using a scanning electron microscope (SEM) equipped with energy-dispersive spectrometer (EDS).

3. Results and discussion

All stepped test castings contained 3.550 wt.% C, 2.110 wt.% Si, 0.098 wt.% Mn, 0.012 wt.% S, 0.035 wt.% P, 0.018 wt.% Cu, 0.029 wt.% Cr, 0.016 wt.% Ni, 0.002 wt.% Mo, 0.048 wt.% Mg, 0.01 wt.% V, 0.0015 wt.% W, 0.0055 wt.% Sn, 0.00041 wt.% Sb, 0.0169 wt.% Ti, 0.0039 wt.% Nb, 0.0029 wt.% Zr, 0.0048 wt.% Ca, 0.00052 wt.% Pb, 0.00015 wt.% As, 0.016 wt.% Co, 0.000017 wt.% Cd, 0.00045 wt.% La, 0.0000038 wt.% Pr, 0.0000017 wt.% Sm, 0.000012 wt.% Nd, 0.000003 wt.% Gd and 0.000014 wt.% Y. Differences in chemical compositions of stepped test castings are shown in Table 2.

TABLE 2

Contents of Ce, Al and Bi in stepped test castings and corresponding values of RE/Bi and RE/SE ratios and K_1 factor

Stepped test casting (STC)	Content of element, wt.%			RE*/Bi	RE/SE**	K_1***
	Ce	Al	Bi			
STC 1	0.0025	0.014	0.000011	270.05	0.144	0.267
STC 2	0.0026	0.0135	0.000011	279.14	0.153	0.266
STC 3	0.0029	0.014	0.00064	5.27	0.159	0.499
STC 4	0.0028	0.018	0.001	3.27	0.128	0.640
STC 5	0.0028	0.016	0.0042	0.78	0.122	1.820

* RE is the total content of rare earth elements (Ce + La + Nd + Pr + Sm + Gd), wt.%

** SE is the total content of subversive elements (Al + As + Sn + Sb +Pb + Bi + Cd), wt.%

*** K_1 is antinodularizing (Thielman) factor (defined by the Eq. (1)).

Achieved Bi contents are very close to the targeted contents (there are no significant deviations). The Si content is in the targeted range. Si is set low because it promotes chunky graphite in thick sections of the casting. RE elements, Ce and La, were purposefully added in a small amount because these elements in combination with Mg increase the nodule count and nodularity in thin sections. The high nodule count is needed in thin sections to prevent carbide formation. All stepped test castings contain a low proportion of elements that promote formation of non-nodular graphite forms, such as Ti, Pb, Sb, As, Cd, Al, *etc.* The content of carbide-promoting elements like Cr, Mn, V, *etc.* is low, which eliminates their influence on the formation of carbides. Antinodularizing (Thielman) factor K_1 (defined by the Eq. (1)) for STC 5 is greater than 1 because of the increased content of Bi.

The results of metallographic analysis show that the section thickness and the Bi content have a great influence on the graphite structure in SGCI castings (Table 3, Figs. 2-5). It can

TABLE 3

Microstructure features of examined stepped test castings

Stepped test casting (STC)	Bi, wt.%	Section thickness, mm	Nodule count	Nodularity, %
STC 1	0.000011	3	488	93.8
		12	393	93.8
		25	168	81.2
		38	161	75.9
		50	115	72.3
		75	66	49.6
		100	94	68.6
STC 2	0.000011 (+ chill)	3	325	92.6
		12	253	88.8
		25	157	80.9
		38	129	79.1
		50	146	79.3
		75	154	83.2
		100	156	78.0
STC 3	0.00064	3	200 (+ carbides)	81.6
		12	291	84.3
		25	297	85.3
		38	195	76.5
		50	109	63.4
		75	107	66.0
		100	90	65.7
STC 4	0.001	3	172 (+ carbides)	83.1
		12	263	88.6
		25	301	87.5
		38	215	79.3
		50	127	65.1
		75	86	63.7
		100	107	68.2
STC 5	0.0042	3	133 (+ carbides)	88.1
		12	382	86.0
		25	379	86.5
		38	324	88.0
		50	304	87.4
		75	192	78.4
		100	270	84.1

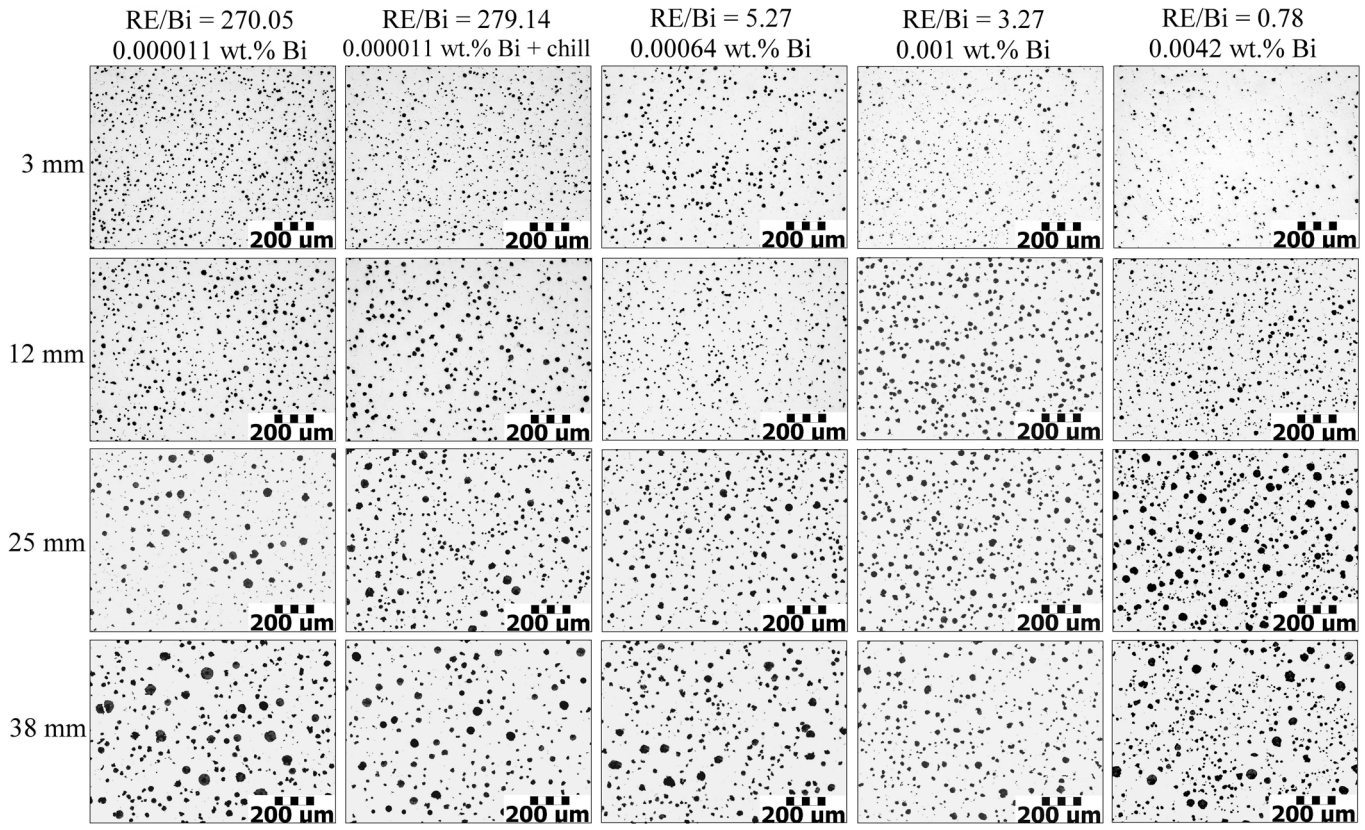

Fig. 2. Optical micrographs of the central part of the section thicknesses of 3, 12, 25 and 38 mm at various contents of Bi, *i.e.*, at various RE/Bi ratios (unetched)

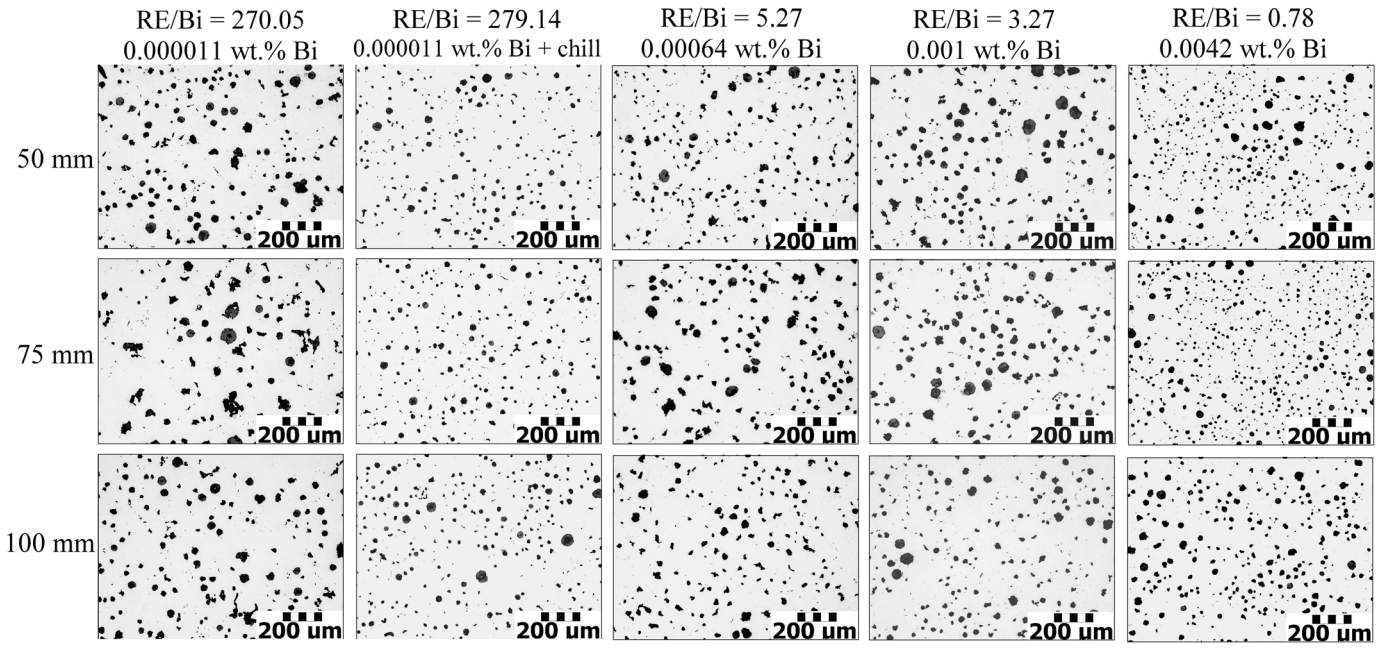

Fig. 3. Optical micrographs of the central part of the section thicknesses of 50, 75 and 100 mm at various contents of Bi, *i.e.*, at various RE/Bi ratios (unetched)

be seen that the nodule count and nodularity increased and size of nodules decreased as the section thickness decreased due to increase in the cooling rate.

In the examined low-silicon SGCI castings, the addition of Bi had a detrimental or beneficial effect, depending on the section thickness. In the section thickness of 3 mm, addition of Bi, *i.e.* decrease in RE/Bi and RE/SE ratios, in all cases resulted in a decrease in nodule count due to the formation of iron carbides (Table 3; Figs. 2 and 6). In STC 1 and STC 2, which were casted without addition of Bi, carbides are not present for this

wall thickness. This clearly shows that Bi affects the formation of carbides in thin walls.

Table 3 and Fig. 2 show that Bi contents ranging from 0.00064 to 0.0042 wt.% did not show a beneficial effect on nodularity and nodule count in the section thickness of 12 mm. The addition of Bi had a positive effect on nodularity and nodule count in section thickness of 25 mm (Table 3; Fig. 2), but was not necessary to achieve nodularity above 80%.

The positive effect of Bi is clearly visible in thicker walls, *i.e.* at lower cooling rates (Table 3; Figs. 2 and 3). In the section thicknesses of 38 and 50 mm, nodularity above 80% was achieved only when 0.0042 wt.% Bi was added (ratio of RE/Bi = 0.78; ratio of RE/SE = 0.122). At the same time, nodule count increased significantly.

The external metallic chill and proper addition of Bi showed a significant positive effect on nodularity and nodule count in section thicknesses of 75 and 100 mm (Table 3; Fig. 3). In STC 1, where chill was not used, nodularity and nodule count were very low due to slow cooling. Increasing the cooling rate by chill in STC 2 resulted in a significant increase in nodularity and nodule count. The additions of 0.00064 and 0.001 wt.% Bi (STC 3 and STC 4) increased very slightly nodularity and nodule count in the section thickness of 75 mm compared to STC 1. These additions did not show a beneficial effect on nodularity and nodule count in the section thickness of 100 mm. It is obvious that these Bi contents were not enough considering the amount of RE elements and the cooling rates. Very high increase in nodularity and nodule count was achieved by addition of 0.0042 wt.% Bi compared to STC 1. Increase of nodularity is comparable with results obtained using the chill. Higher nodule count was obtained by addition of 0.0042 wt.% Bi than by using the chill. These results suggest that an additional increase in the nucleation potential of the melt by proper addition of Bi shows a significantly greater effect on the graphite structure and the number of graphite particles at lower cooling rate.

4. Conclusion

Obtained results show that the chemical composition and the cooling rate during solidification significantly affected the graphite structure in the examined ductile iron castings containing 2.11 wt.% Si and RE elements (Ce + La + Nd + Pr + Sm + Gd) in the range from 0.00297 to 0.00337 wt.%. Nodules count increased

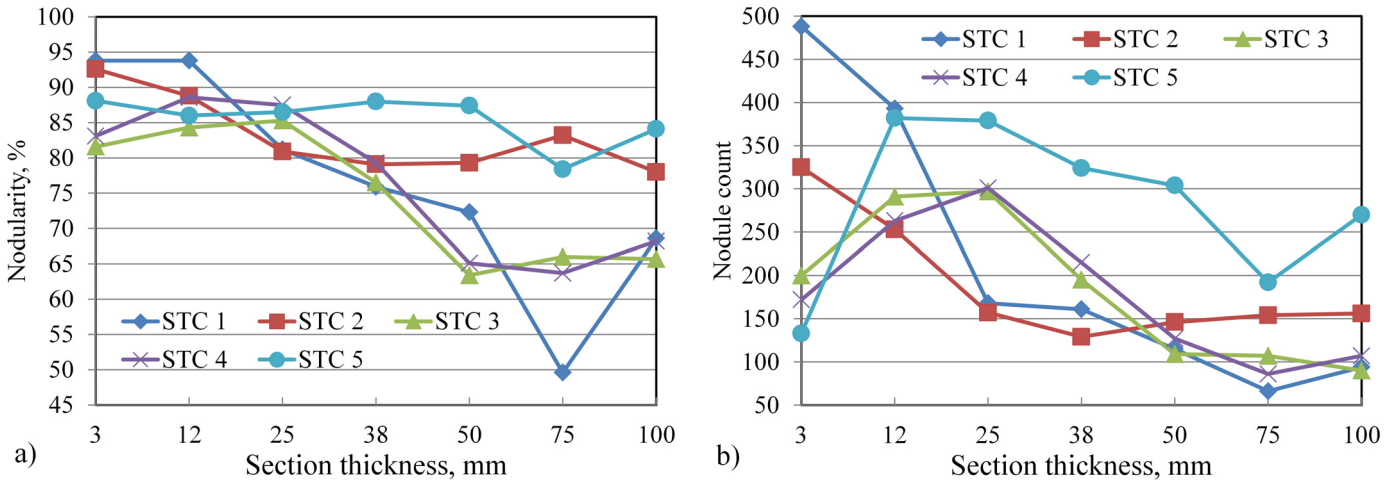

Fig. 4. Effect of section thickness in stepped test casting on nodularity (a) and the nodule count (b)

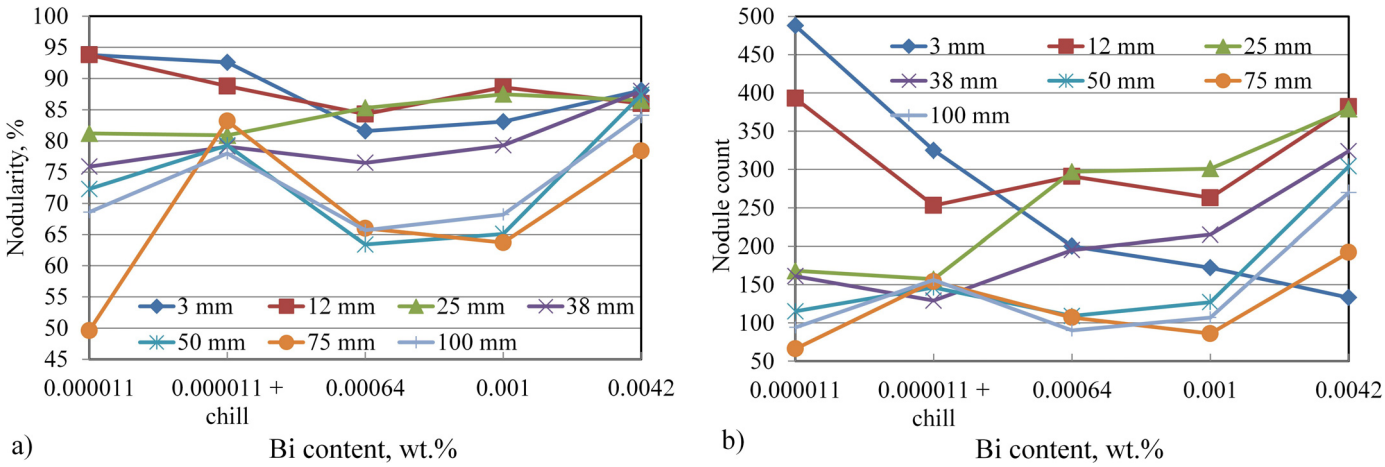

Fig. 5. Effect of Bi addition on nodularity (a) and the nodule count (b) in the section thicknesses of 3, 12, 25, 38, 50, 75 and 100 mm

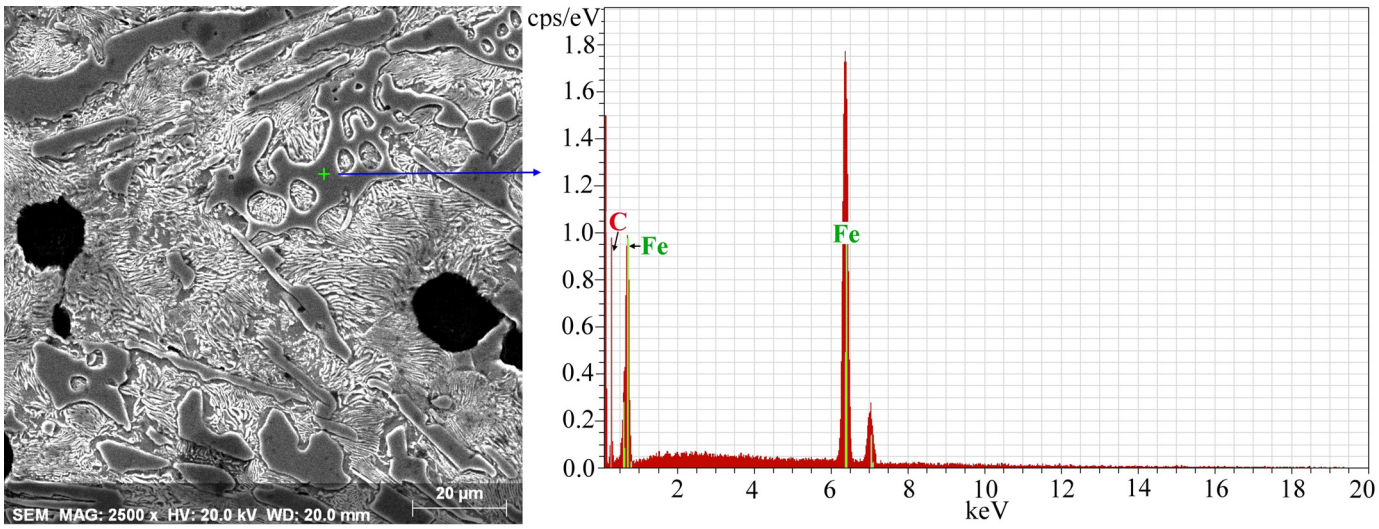

Fig. 6. SEM-EDS point analysis of carbides which were found in the section thickness of 3 mm in STC 5

and their size decreased with the increasing cooling rate, *i.e.*, with the decreasing section thickness, due to an increase in undercooling and nucleation rate of graphite during solidification.

Nodularity above 90% and a very high nodule count were achieved in the section thicknesses of 3 and 12 mm without the addition of Bi and the application of external metallic chill in the mold. This is the result of high nucleating potential of the melt, appropriate content of RE elements for these sections, high cooling rate and low contents of antinodularizing elements. The additions of 0.00064, 0.001 and 0.0042 wt.% Bi, *i.e.*, decrease in RE/Bi and RE/SE ratio resulted in a decrease in nodule count in the section thickness of 3 mm due to the formation of iron carbides. This indicates that Bi promotes the formation of iron carbides in very thin sections when the Si content is low.

Nodularity slightly above 80% and a relatively high nodule count were achieved in the section thickness of 25 mm without the addition of Bi and the use of chill. This suggests that the high metallurgical melt quality allows the achievement of favorable microstructural features in this medium-thick section. However, the additions of 0.00064, 0.001 and 0.0042 wt.% Bi resulted in an increase in nodularity slightly above 85%. Nodule count was significantly increased by the addition of Bi. It is obvious that Bi improves the nucleation potential of SGCI melt containing RE elements. This effect of Bi becomes more pronounced at slower cooling.

In the section thicknesses of 38, 50, 75 and 100 mm nodularity above 80% was not obtained without the appropriate addition of Bi or the use of chill. Slow cooling resulted in the formation of non-spheroidal graphite particles. It was found that the number of non-spheroidal graphite particles increased with increasing section thickness, *i.e.*, with decreasing cooling rate. Harmful effect of RE elements in these sections was neutralized by adequate addition of Bi. This resulted in an increase in nucleation potential of melt, nodule count and nodularity and decreasing number of non-spheroidal graphite particles. Bi content of 0.001 wt.% (ratio of RE/Bi = 3.27; ratio of RE/SE = 0.128) was sufficient to obtain nodularity above 80% and high nodule count in the section thickness of 38 mm. High nodule count and nodularity above 80% in the section thicknesses of 50, 75 and 100 mm were achieved by the addition of 0.0042 wt.% Bi (ratio of RE/Bi = 0.78; ratio of RE/SE = 0.122). The obtained results indicate that Bi can significantly increase the nodule count and nodularity in medium-thick and thick sections of SGCI castings. In order to obtain the maximum effect, the addition of Bi must be adjusted to the amount of RE elements and the section thickness of the casting. The required addition of Bi increases with an increase in content of RE elements and section thickness of the casting. Excessive additions of Bi may have a detrimental effect on the graphite structure in SGCI castings.

Results of this research show that the solidification rate of the thick sections can be increased by placing the external metallic chill in the appropriate place in the mold. In this case, addition of Bi is not required to achieve high nodule count and nodularity.

REFERENCES

[1] S. Komatsu, T. Shiota, T. Matsuoka, K. Nakamura, AFS Trans. **102**, 121-125 (1994).
[2] P. Ferro, P. Lazzarin, F. Berto, Mater. Sci. Eng. A **554**, 122-128 (2012).
[3] I. Riposan, M. Chisamera, A. Stan, Int. J. Metalcast. **7** (1), 9-20 (2013).
[4] C. Labrecque, P.M. Cabanne, China Foundry **8** (1), 66-73 (2011).
[5] S. Hasse, Giesserei-Prax. 15/16, 271-278 (1995).
[6] I. Riposan, M. Chisamera, V. Uta, S. Stan, Int. J. Metalcast. **8** (2), 65-80 (2014).
[7] I. Riposan, M. Chisamera, S. Stan, China Foundry **7** (2), 163-170 (2010).
[8] M.I. Onsøien, Ø. Grong, T. Skaland, K. Jørgensen, Mater. Sci. Technol. **15** (3), 253-259 (1999).
[9] J.O. Choi, J.Y. Kim, C.O. Choi, J.K. Kim, P.K. Rohatgi, Mater. Sci. Eng. A, **383**, 323-333 (2004).

[10] Z. Jiyang, China Foundry, **7** (2), 183-198 (2010).
[11] P. Ferro, A. Fabrizi, R. Cervo, C. Carollo, J. Mater. Process. Technol. 213 (9), 1601-1608 (2013).
[12] Z. Zhang, H.M. Flower, Y. Niu, Mater. Sci. Techol. **5** (7), 657-664 (1989).
[13] H. Itofiji, H. Uchikawa, AFS Trans. **98**, 429-448 (1990).
[14] N. Yingyi, Z. Zhu, Foundryman **81** (8), 390-398 (1988).
[15] R. Källbom, K. Hamberg, M. Wessén, L.E. Björkegren, Mater. Sci. Eng. A **413-414**, 346-351 (2005).
[16] H. Morrogh, AFS Trans. **60**, 439-452 (1952).
[17] G.S. Cole, AFS Trans. **80**, 335-348 (1972).
[18] J. Verelst, A. DeSy, Giesserei **43** (12), 305-315 (1956).
[19] I. Aoki, T. Tottori, Iron Steel **43** (11), 1191-194 (1957).
[20] H. Takeda, H. Yoneada, K. Asano, Mater. Trans. **51** (1), 176-185 (2010).
[21] H. Takeda, K. Asano, H. Yoneada, Int. J. Cast Met. Res. **21** (1-4), 81-85 (2008).
[22] H. Horie, T. Kowata, A. Chida, Cast Met. **2** (4), 197-202 (1990).
[23] W. Shihe, X. Guoqing, D. Hanqiao, L. Hantong, in Proceedings of the fourth International Symposium on the physical metallurgy of cast iron, eds. G. Ohira, T. Kusakawa, E. Niyama, Tokyo, Japan, 119-124 (1989).
[24] A. Javaid, C.R. Loper, Jr, AFS Trans. **103**, 135-150 (1995).
[25] E.N. Pan, C.Y. Chen, AFS Trans. **104**, 845-858 (1996).
[26] Z. Jiyang, China Foundry **7** (1), 76-88 (2010).
[27] Z. Bofan, E.W. Langer, Scand. J. Metall. **13**, 15-22 (1984).
[28] M.N. Abdusalyamova, A.G. Chuiko, E.I. Shishkin, O.I. Rachmatov, J. Alloys Compd. **240**, 272-277 (1996).
[29] Z. Jiyang, W. Schmitz, S. Engler, AFS Trans. **98**, 783-786 (1990).
[30] B. Lux, Giessereiforschung **2**, 65-80 (1970).
[31] D.K. Banerjee, D.M. Stefanescu, AFS Trans. **99**, 747-759 (1991).
[32] Z. Jiyang, China Foundry, **7** (3), 292-307 (2010).
[33] Z. Jiyang, China Foundry, **7** (4), 470-478 (2010).
[34] ASTM E2567-14: Standard Test Method for Determining Nodularity and Nodule Count in Ductile Iron Using Image Analysis, ASTM International, USA, 1-4 (2014).